Available online at www.sciencedirect.com
SCIENCE DIRECT
Bioorganic & Medicinal Chemistry 14 (2006) 1880–1888
Bioorganic & Medicinal Chemistry

Synthesis, characterization, cytotoxic activities, and DNA-binding properties of the La(III) complex with Naringenin Schiff-base

Bao-dui Wang,[a] Zheng-Yin Yang,[a,*] Qin Wang,[b] Ti-kuan Cai[b] and Patrick Crewdson[c]

[a]*College of Chemistry and Chemical Engineering and State Key Laboratory of Applied Organic Chemistry, Lanzhou University, Lanzhou 730000, PR China*
[b]*College of life science, Department of Chemistry, Lanzhou University, Lanzhou 730000, PR China*
[c]*Department of Chemistry, University of Ottawa, Ottawa, Ont., Canada K1N 6N5*

Received 9 August 2005; revised 20 October 2005; accepted 21 October 2005
Available online 28 November 2005

Abstract—A new Naringenin Schiff-base ligand (H_3L) and its complex, $[La(H_2L)_2(NO_3)\cdot 3H_2O]$, have been synthesized and characterized on the basis of elemental analyses, molar conductivities, mass spectra, ^1H NMR, thermogravimetry/differential thermal analysis (TG–DTA), UV spectra, and IR spectra. Spectrometric titrations, ethidium bromide displacement experiments, and viscosity measurements indicate that the two compounds, especially the La(III) complex, strongly bind with calf-thymus DNA, presumably via an intercalation mechanism. The intrinsic binding constants of the La(III) complex and ligand with DNA were 1.83×10^7 and $9.46 \times 10^5\ M^{-1}$, respectively. Comparative cytotoxic activities of the La(III) complex and ligand were also determined by MTT [3-(4,5-dimethyl-2-thiazoyl)-2,5-diphenyl-2*H*-tetrazolium bromide] and SRB (sulforhodamine B) methods. The results showed that the La(III) complex had significant cytotoxic activity against the tested cells.

1. Introduction

Numerous biological experiments have demonstrated that DNA is the primary intracellular target of anticancer drugs due to the interaction between small molecules and DNA, which cause DNA damage in cancer cells, blocking the division of cancer cells and resulting in cell death.[1–3] Of these studies, the interaction of transition metal complexes containing multidentate aromatic ligands with DNA has gained much attention. This is due to their possible application as new therapeutic agents and their photochemical properties which make them potential probes of DNA structure and conformation.[4–9]

The design of small complexes that bind and react at specific sequences of DNA becomes important. A more complete understanding of how to target DNA sites with specificity will lead not only to novel chemotherapeutics but also to a greatly expand ability for chemists to probe DNA and to develop highly sensitive diagnostic agents.[4]

Transition-metal complexes are being used at the forefront of many of these efforts. Stable, inert, and water-soluble complexes containing spectroscopically active metal centers are extremely valuable as probes of biological systems. As both spectroscopic tags and functional models for the active centers of proteins, metal complexes have helped elucidate the mechanisms by which metalloproteins function.[4]

In order to develop new antitumor drugs which specifically target DNA, it is necessary to understand the different binding modes a complex is capable of undertaking. Basically, metal complexes interact with the double helix DNA in either a non-covalent or a covalent way. The former way includes three binding modes: intercalation, groove binding, and external static electronic effects. Among these interactions, intercalation is one of the most important DNA binding modes as it invariably leads to cellular degradation. It was reported that the intercalating ability increases with the planarity of ligands.[10,11] (Additionally, the coordination

Keywords: Naringenin Schiff-base; La(III) complex; Cytotoxic activities; DNA binding.
* Corresponding author. Fax: +86 931 8912582; e-mail: yangzy@lzu.edu.cn

0968-0896/$ - see front matter © 2005 Elsevier Ltd. All rights reserved.
doi:10.1016/j.bmc.2005.10.031

geometry and ligand donor atom type also play key roles in determining the binding extent of complexes to DNA.)[12,13] The metal ion type and its valence, which are responsible for the geometry of complexes, also affect the intercalating ability of metal complexes to DNA.[14,15]

Flavonoids are a broadly distributed class of naturally occurring pigments present in vascular plants and are responsible for most of the colors in nature. These natural products are potentially antibacterial, anticancer, antioxidant, anti-inflammatory, and antiallergenic agents since they stimulate or inhibit a wide variety of enzyme systems as pharmacological agents.[16–21] The best known flavonoids, such as quercetin, morin, and rutin, have been studied previously.[22,23] Naringenin is one of the lesser-known flavonoids expect for its use as antibacterial and anticancer agents.[24] In addition, some hydrazones and their complexes with metals often have diverse biological and pharmaceutical activities.[25–30] However, up to now the biological activity and interactions of naringenin hydrazones and their complexes with DNA have not been reported. This aroused our interest in the synthesis of a new ligand, 4′,5,7-trihydroxy-flavanoe benzoyl hydrazone (H_3L), and its La(III) complex in view of evaluating their pharmaceutical activities. The ligand was prepared by the reaction shown in Figure 1.

2. Results

The complex is air stable for extended periods and soluble in methanol, DMSO, and DMF; slightly soluble in ethanol; insoluble in benzene, water, and diethyl ether. The molar conductance value is 54.7 $ohm^{-1}\,mol^{-1}\,cm^2$ in DMF, showing that the complex is non-electrolytic in DMF.[31] The elemental analyses suggest that the formula of the complex is $[La(H_2L)_2(NO_3)\cdot 3H_2O]$. The complex exhibits its first endothermic peak at 58.4 °C in the TG–DAT (Fig. S3), which corresponds to 5.45%, a value that indicates three water molecules.

2.1. IR spectra

The ν(C=O) vibration of the free ligand is at 1640 cm^{-1}; for the complex the peak shifts to 1609 cm^{-1}, $\Delta\nu_{(ligand-complex)}$ is equal to 31 cm^{-1}. A band, which appears at 470 cm^{-1} after reaction with the metal, is assigned to ν(M–O). These data indicate that the oxygen of the carbonyl has likely formed a coordination bond with the rare earth ion.[32] The band at 1600 cm^{-1} for the free ligand is assigned to ν(C=N); for the complex the peak shifts to 1570 cm^{-1}, $\Delta\nu_{(ligand-complex)}$ is equal to 30 cm^{-1}. A weak band appearing at 413 cm^{-1} is assigned to ν(M–N). These data would indicate that the nitrogen of the imino group also bonds to the rare earth ion.[33] The aqueous ν(OH) and δ(HOH) bands of the complex appear at 3399 and 1594 cm^{-1}, respectively, showing that there is some water in the complex.[34] For the free ligand, ν(NH) and δ (NNH) appear at 3205 and 1520 cm^{-1}; the two bands for the complex shift to 3228 and 1543 cm^{-1}, respectively, which demonstrates that there is one hydrogen of the =NNH– in the complex. All of these data confirm the fact that a conjugate chelate ring formed by ligand-enolization exists in the complex. The absorption bands assigned to the coordinated nitrates were observed at about 1489 (ν_{as}) and 893 (ν_s) cm^{-1}. The separation of the two highest frequency bands $|\nu_4 - \nu_1|$ is approximately 176 cm^{-1}, and accordingly the coordinated NO_3^- ion in the complex is a bidentate ligand.[35]

2.2. ^{1}H NMR spectra

The ^{1}H NMR spectra of the ligand (Fig. S1) and its La(III) complex (Fig. S2) are assigned as follows: H_2L ($(CD_3)_2CO$), δ (ppm): 2.97 (1H, dd, J = 12.3, 17.0 Hz, 3(a)-H), 3.46 (1H, dd, J = 3.0, 17.0 Hz, 3(e)-H), 5.11 (1H, dd, J = 3.0, 12.3 Hz, 2(a)-H), 5.95 (1H, d, J = 4.8 Hz, 6-H), 5.98 (1H, d, J = 4.8 Hz, 8-H) 6.90 (2H, d, J = 8.4 Hz, 3′, 5′-H), 7.36–7.55 (5H, m, PhH), 7.92 (2H, d, J = 8.4 Hz, 2′, 6′-H), 9.04 (1H, s, 4-OH), 9.50 (1H, s, 7-OH), 10.52 (1H, s, 5-OH), 13.08 (1H, s, –NH–C=O). La $(H_2L)_2(NO_3)\cdot 3H_2O$ (DMSO-d_6), 2.89 (2H, d, J = 9.0 Hz, 3(a)-H), 3.53-3.80 (6H, br, H_2O), 3.86 (2H, d, J = 9.0 Hz, 3(e)-H), 5.00 (2H, br, 2(a)-H), 5.49 (2H, J = 9.6 Hz, 6-H), 5.90 (2H, d, J = 9.6 Hz, 8-H), 6.78 (4H, d, J = 10.5 Hz, 3′, 5′-H), 7.24–7.60 (10H, m, PhH), 7.90 (4H, d, J = 10.5 Hz, 2′, 6′-H), 9.18 (2H, s, 4-OH), 9.58 (2H, s, 7-OH), 13.16 (2H, s, –NH–C=O–). In the complex, the –OH-5 hydrogen is replaced by metal and the –NH– group of the complex shifts downfield (9.58 ppm) compared to that of the free ligand. The hydrogen of the =NNH– group is still detected in the complex, which is also supported by the IR spectra.

2.3. Electronic absorption titration

The study of the electronic spectra in the ultraviolet and visible ranges for the La(III) complex and ligand was carried out in a buffer solution. The electronic spectra of ligand had a strong band at λ_{max} = 201 nm, a medium band at λ_{max} = 323 nm and a weak band at λ_{max} = 223 nm. It follows from the literature that the band at 323 nm is related to the absorbance of the B ring

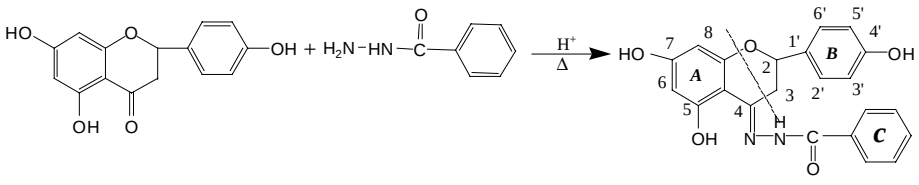

Figure 1. Preparation route of the ligand (H_3L).

(cinnamoyl system), whereas the band at 201 nm is related to the $\pi \rightarrow \pi^*$ transition absorbance (benzoyl system) in the A ring. The band at 223 nm is the absorbance of the C ring.[36] The spectra of the La complex were the same, except for the peak at 323 nm, which is shifted to 335 nm.

The absorption spectra of the La(III) complex and ligand in the absence and presence of CT-DNA (at a constant concentration of compound) are given in Figure 2. In the presence of CT-DNA, the absorption bands of La(III) complex at about 202 nm and 335 nm exhibited hypochromism of about 47.28% and 17.51%, and bathochromism of about 13 and 3 nm, respectively. The ligand at 201 and 323 nm exhibits hypochromism of about 37.53% and 11.42%, and bathochromism of about 7 and 1 nm. It is noteworthy that the hypochromicity of the complex is much greater than that of the parent ligand.

2.4. Fluorescence spectra

The La(III) complex and ligand can emit weak luminescence in Tris buffer with a max wavelength of about 446 nm. The results of the emission titrations for the La(III) complex and ligand with DNA are illustrated in the titration curves (Fig. 3). Upon addition of DNA, for the La(III) complex and ligand, the emission intensities of the compounds grow to around 3.78 and 4.53 times larger, respectively, than those in the absence of DNA.

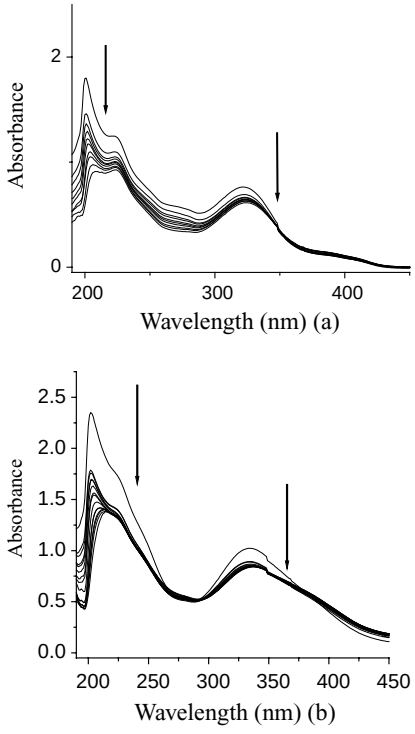

Figure 2. (a) Electronic spectra of ligand (10 μM) in the presence of increasing amounts of CT-DNA. [DNA] = 0–22.25 μM. Arrow shows the absorbance changes upon increasing DNA concentration. (b) Electronic spectra of La(III) complex (10 M) in the presence of increasing amounts of CT-DNA. [DNA] = 0–22.5 μM. Arrow shows the absorbance changes upon increasing DNA concentration.

Steady-state emission quenching experiments are also used to observe the binding mode of the compounds to DNA. Figure 4 shows the emission spectra of the DNA–EB system with increasing amounts of La(III) complex and free ligand. The emission intensity of the DNA–EB system (λ = 578 nm) decreased as the concentration of the La(III) complex and ligand increased, and an isobathic point appeared at 555 nm. The quenching plots illustrate that the quenching of EB bound to DNA by the ligand and the complex is in good agreement with the linear Stern–Volmer equation.

2.5. Viscosity studies

The effects of both compounds on the viscosity of DNA are shown in Figure 5. The viscosities of the DNA increase steadily with increasing concentration of ligand and La(III) complex, and the extent of the increase observed for the ligand is smaller than that for the La(III) complex.

2.6. Cytotoxic activity

The cytotoxicity assays of the La(III) complex and ligand against two kinds of tumor cells (human leukemia HL-60 and lung adenocarinoma A-549) are shown in Figures 6 and 7. The La(III) complex exhibited activity higher than that of the free ligand at all concentrations. At a concentration of 10^{-9} mol L^{-1}, the La(III) complex showed an inhibition rate of over 50% against human leukemia HL-60. For the A-549 cell line the La(III) complex demonstrated a stronger inhibitory effect than even cisplatin[37] over a range of concentrations from 10^{-5} to 10^{-8} mol L^{-1}.

3. Discussion

3.1. Structure of the La(III) complex

Since the crystal structure of the La(III) complex has not been obtained yet, we characterized the complex and determined its possible structure by elemental analyses, molar conductivities, ^{1}H NMR, IR data, TG–DTA, and UV–vis measurements. The likely structure of the complex is shown in Figure 8.

3.2. DNA-binding constant and mode

The interactions of metal complexes with DNA have been the subject of interest for the development of effective chemotherapeutic agents. Transition metal centers are particularly attractive moieties for such research since they exhibit well-defined coordination geometries and also often possess distinctive electrochemical or photophysical properties, thus enhancing the functionality of the binding agent.[5]

Electronic absorption spectroscopy was an effective method in examining the binding mode of DNA with the metal complex.[38–40] If the binding mode was intercalation, the π^* orbital of intercalated ligand can couple with the π orbital of the base pairs, thus decreasing

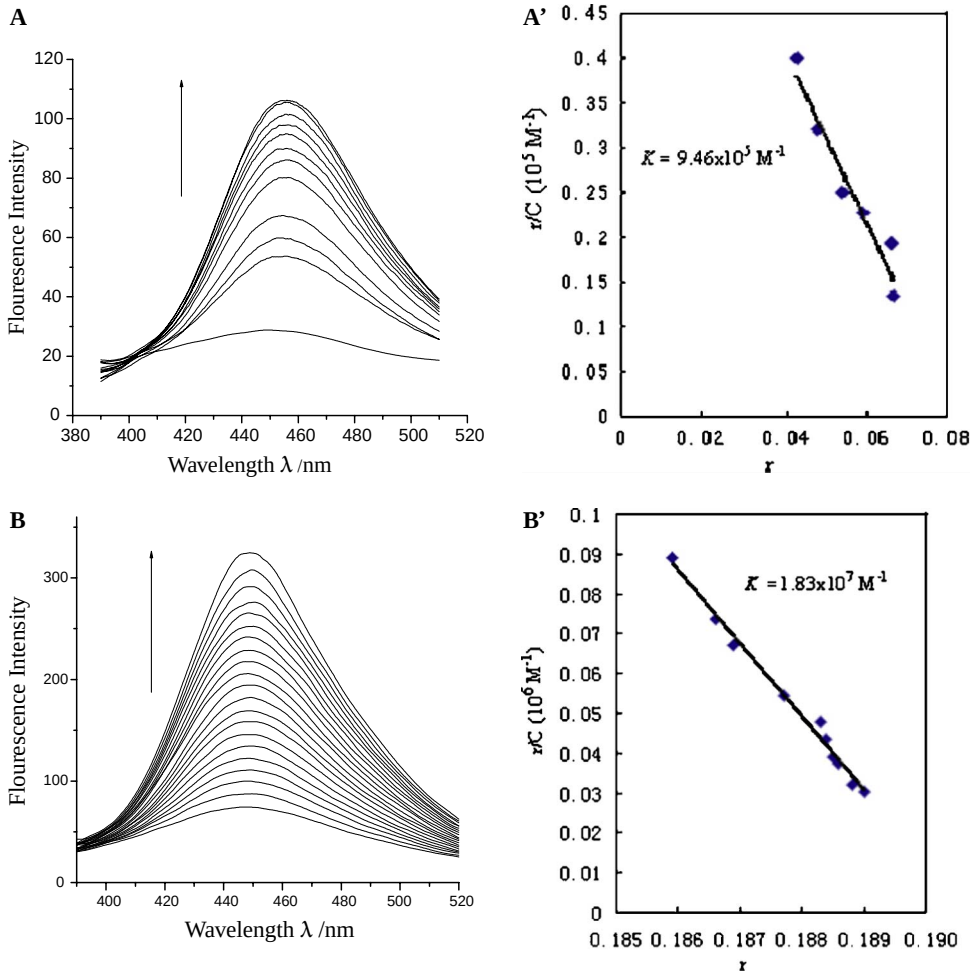

Figure 3. (A) The emission enhancement spectra of ligand (10 μM) in the presence of 0, 2.5, 5, 7.5, 10, 12.5, 15, 17.5, 20, and 22.5 μM CT-DNA. Arrow shows the emission intensity changes upon increasing DNA concentration. Inset: Scatchard plot of the fluorescence titration data of ligand, $K = 9.46 \times 10^5\ M^{-1}$. (B) The emission enhancement spectra of the La(III) complex (10 μM) in the presence of 0, 2.5, 5, 7.5, 10, 12.5, 15, 17.5, 20, 22.5, 25, 27.5, 30, 32.5, 35, and 37.5 μM CT-DNA. Arrow shows the emission intensities upon increasing DNA concentration. Inset: Scatchard plot of the fluorescence titration data of the La(III) complex, $K = 1.83 \times 10^7\ M^{-1}$.

the $\pi \rightarrow \pi^*$ transition energy and resulting in bathochromism. If the coupling π orbital is partially filled by electrons, it results in decreasing the transition probabilities and concomitantly results in hypochromism.[41]

The spectroscopic variations are strongly indicative of the intercalation of the La(III) complex and the ligand with CT DNA, involving a strong π-stacking interaction between the complex (or ligand) and the DNA base pairs. They can both insert into DNA base pairs, but it appears that the complex inserts into DNA more deeply. Since the hypochromism of the $\pi \rightarrow \pi^*$ transition absorbance (benzoyl system) in the A ring is greater than those of B ring and C ring, we deduced that the A ring intercalates deeply into the DNA base pairs, whereas the B ring interacts with DNA through a semi-intercalation or quasi-intercalation.[42]

In order to test if the La(III) complex could bind to DNA by intercalation, ethidium bromide (EB) was employed, as EB interacts with DNA as a typical indicator of intercalation.[43] Figure 9 shows that the maximal absorption of EB at 479 nm decreased and shifted to 515 nm in the presence of DNA, which is characteristic of intercalation. Figure 9c is the absorption of a mixture solution of EB, La(III) complex, and DNA. It was found that the absorption at 515 nm increased compared with Figure 9b. This could result from two reasons: (1) EB bound to the La(III) complex strongly, resulting in a decreased amount of EB intercalated into DNA; (2) there exists competitive intercalation between the La(III) complex and EB with DNA, thus releasing some free EB from the DNA–EB system. However, the former reason could be precluded since there were no new absorption peaks.

The results of the emission titrations suggest that both the compounds are protected from solvent water molecules by the hydrophobic environment inside the DNA helix, and that the complex can be protected more efficiently than the free ligand. This implies that both the compounds can insert between DNA base pairs deeply and that the complex can bind to DNA more strongly than just the free ligand. Since the hydrophobic environ-

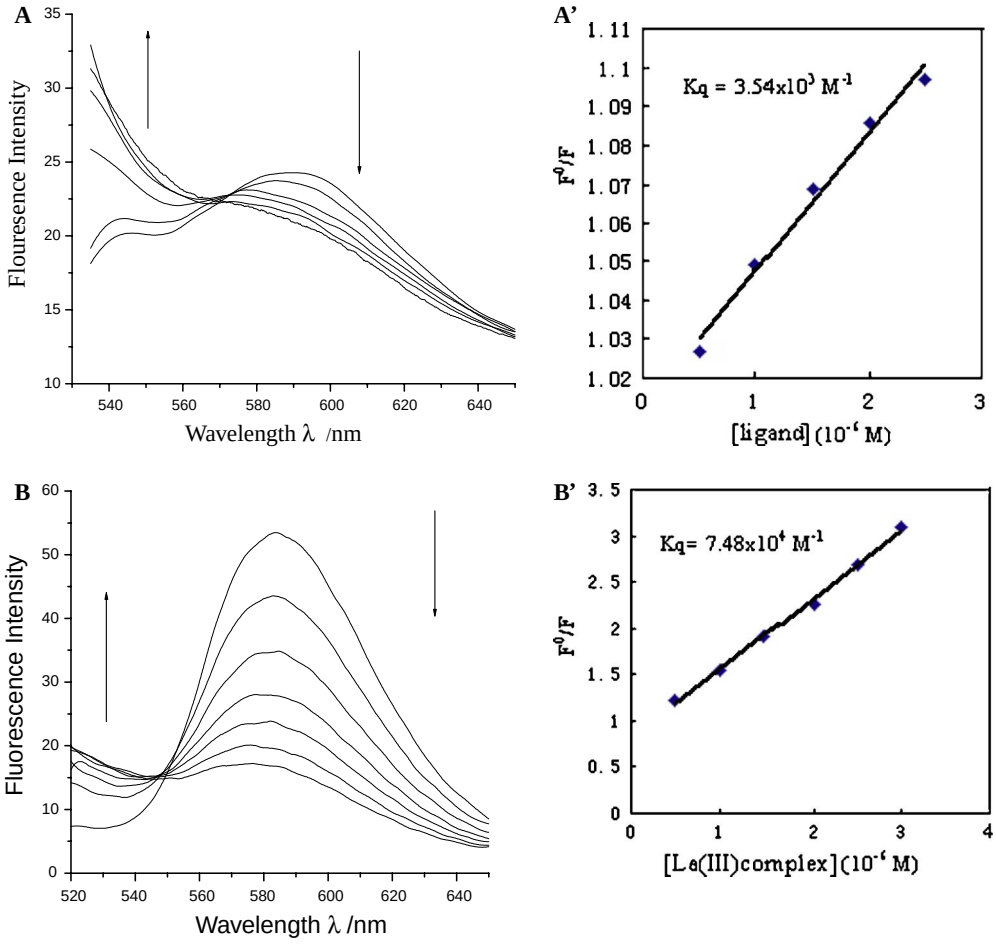

Figure 4. (A) The emission spectra of DNA-EB system (10 μM and 0.32 μM EB), λ_{ex} = 500 nm, λ_{em} = 520.0–650.0 nm, in the presence of 0, 5,10, 15, 20, 25, and 30 μM ligand. Arrow shows the emission intensity changes upon increasing ligand concentration. Inset: Stern–Volmer plot of the fluorescence titration data of ligand, $K_q = 3.54 \times 10^3\ M^{-1}$. (B) The emission spectra of DNA–EB system (10 and 0.32 μM EB), λ_{ex} = 500 nm, λ_{em} = 520.0–650.0 nm, in the presence of 0, 5, 10, 15, 20, 25, and 30 μM La(III) complex. Arrow shows the emission intensity changes upon increasing La(III) complex concentration. Inset: Stern–Volmer plot of the fluorescence

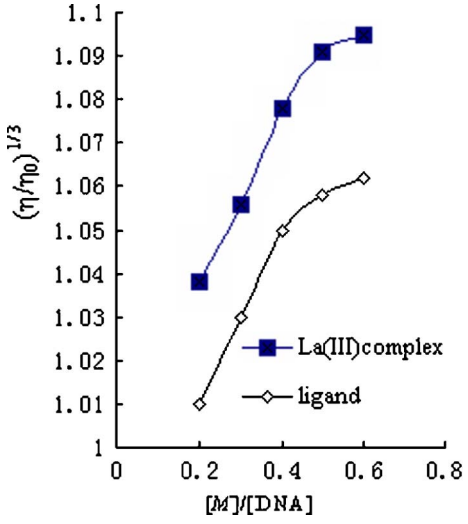

Figure 5. Effect of increasing amounts of La(III) complex and ligand on the relative viscosity of caltf thymus DNA at 25.0 °C.

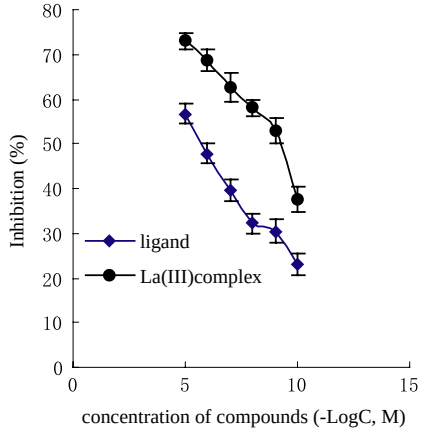

Figure 6. Cytotoxic activity of compounds against HL-60.

ment inside the DNA helix reduces the accessibility of solvent water molecules to the compound and the compound mobility is restricted at the binding site, a decrease of the vibrational modes of relaxation results. The binding of the La(III) complex and ligand to

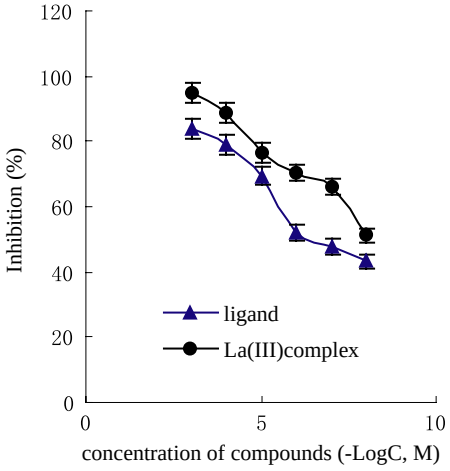

Figure 7. Cytotoxic activity of compounds against A-549.

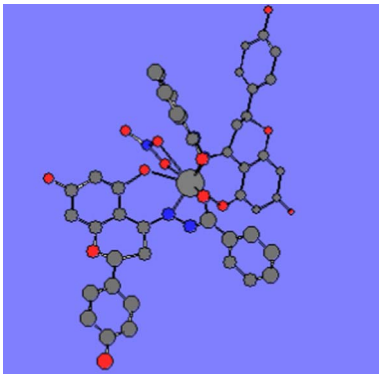

Figure 8. The suggested structure of the complex.

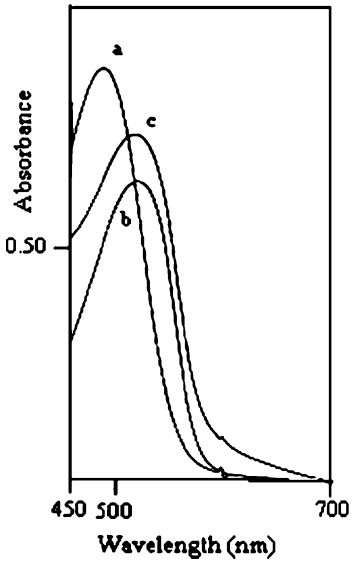

Figure 9. The visible absorption spectra of 1×10^{-5} M EB (a); (a) $+1 \times 10^{-4}$ M DNA (b); (b) $+3 \times 10^{-4}$ La(III) complex; (c) in Tris–HCl buffer (5 mM Tris–HCl, 50 mM NaCl, pH 7.1) solution.

DNA leads to a marked increase in emission intensity, which also agrees with those observed for other intercalators.[44] According to the Scatchard equation, a plot of r/C_f versus r gave the binding constants 1.83×10^7 and 9.46×10^5 M^{-1} from the fluorescence data for the La(III) complex and the free ligand, respectively. These results show that the complex binds more strongly than the free ligand. The higher binding affinity of complex is probably attributed to the extension of the π system of the intercalated ligand due to the coordination of La, which also leads to a planar area greater than that of the free ligand, which leads to the coordinated ligand penetrating more deeply into, and stacking more strongly with the base pairs of the DNA.

The DNA-binding modes of both compounds were further monitored by a fluorescent EB displacement assay.[45] It is well known that EB can intercalate nonspecifically into DNA which causes it to fluoresce strongly. Competitive binding of other drugs to DNA and EB will result in displacement of bound EB and a decrease in the fluorescence intensity. This fluorescence-based competition technique can provide indirect evidence for the DNA-binding mode. The emission band at 578 nm of the DNA–EB system decreased in intensity with an increase in the concentration of the two compounds, which indicated that the compounds could displace EB from the DNA–EB system. The resulting decrease in fluorescence was caused by EB changing from a hydrophobic environment to an aqueous environment.[46] Such a characteristic change is often observed in intercalative DNA interactions.[47] The quenching plots illustrate that the quenching of EB bound to DNA by the ligand and complex is in good agreement with the linear Stern–Volmer equation. In the plots of F_0/F versus [Q], K_q is given by the ratio of the slope to the intercept. The K_q values for the La(III) complex and ligand are 7.48×10^4 and 3.54×10^3 M^{-1}, respectively. The data show that the interaction of the La(III) complex with DNA is stronger than that of the free ligand, which is consistent with the above absorption spectral results. Since these changes indicate only one kind of quenching process, it may be concluded that the La(III) complex and free ligand bind DNA via the same mode (intercalation mode).

Optical photophysical probes generally provide necessary, but not sufficient, clues to support one binding mode. Hydrodynamic measurements that are sensitive to the length change (i.e., viscosity and sedimentation) are regarded as the least ambiguous and most critical tests for binding in solution in the absence of crystallographic structural data.[48] A classical intercalation model demands that the DNA helix lengthen as base pairs are separated to accommodate the binding ligand, leading to an increase in DNA viscosity. In contrast, a partial, non-classical intercalation of compound could bend (or kink) the DNA helix, reducing its effective length and, concomitantly, its viscosity.[49,50] Viscosity experimental results clearly show that both the compounds can intercalate between adjacent DNA base pairs, causing an extension in the helix, and thus increase the viscosity of DNA; and that the La(III) complex can intercalate more strongly and deeply than the free ligand, leading to the greater increase in viscosity of the DNA with an increasing concentration of complex.

The results obtained from viscosity studies validate those obtained from the spectroscopic studies.

On the basis of all the spectroscopic studies together with the viscosity measurements, we come to the conclusion that the La(III) complex and ligand can bind to CT-DNA in an intercalative mode and that the La(III) complex binds to CT-DNA more strongly than the free ligand.

3.3. Bioassay in vitro

The inhibitory rate of the La(III) complex is much higher than that of the free ligand, which may be attributed to the extended planar structure induced by the p−π* conjugation resulting from the chelation of the metal ion with the ligand. Moreover, the inhibitory effect of the La(III) complex was higher than that of cisplatin against the A-549 cell line at some experimental concentrations. These findings of cytotoxic activity in vitro prompted us to explore the DNA-binding studies on this compound.

4. Conclusion

Taken together, a new ligand, 4′,5,7-trihydroxy-flavanoe benzoyl hydrazone (H_3L), and its La(III) complex have been prepared and characterized. The DNA-binding properties of the ligand and La(III) complex were investigated by absorption, fluorescence, and viscosity measurements. The results support the fact that both the compounds bind to CT-DNA via intercalation. The binding constant shows that the DNA-binding affinity increases in the order: free ligand < La(III) complex. The two compounds have shown considerable cytotoxic activity against two tumor cell lines, and the suppression rate of the La(III) complex is higher than that of the ligand itself. The La(III) complex against the A-549 cell line was more potent than cisplatin at most experimental concentrations. These findings can shed some light on designing new potent anticancer drugs.

5. Experimental

5.1. Materials

DNA and EB (ethidium bromide) were purchased from Sigma Chemical Co. Naringenin was produced in Hui Ke Co. (P.R.C.). Benzoyl hydrazine was produced by the Shang Hai Reagent Co (P.R.C.). All chemicals used were of analytical grade. The La(III) nitrate was prepared from its oxide (99.9%) acquired from Nong Hua (P.R.C.). All the experiments involving interaction of the La(III) complex and the ligand with DNA were carried out in doubly distilled water buffer containing 5 mM Tris [Tris(hydroxymethyl)-aminomethane] and 50 mM NaCl, and adjusted to pH 7.1 with hydrochloric acid. A solution of CT-DNA in the buffer gave a ratio of UV absorbance of about 1.8–1.9:1 at 260 and 280 nm, indicating that the DNA was sufficiently free of protein.[51] The DNA concentration per nucleotide was determined by absorption spectroscopy using the molar absorption coefficient (6600 $M^{-1}\,cm^{-1}$) at 260 nm.[52] The ligand and the La(III) complex were dissolved in a mixture solvent of 1% CH_3OH and 99% Tris–HCl buffer (5 mM Tris–HCl, 50 mM NaCl, pH 7.1) at concentration 1.0×10^{-5} M.

5.2. Measurements

Carbon, hydrogen, and nitrogen were analyzed on an Elemental Vario EL analyzer. The metal contents of the complex were determined by titration with EDTA. Infrared spectra (4000–400 cm^{-1}) were determined with KBr disks on a Therrno Mattson FTIR spectrometer. The ultraviolet spectra were recorded on a Varian Cary 100 Conc spectrophotometer. The thermal behavior was monitored on a Beijing Optics Instrument Factory PCT-2 differential thermal analyzer. The molar conductance values were determined in DMF on a Shanghai Leici DSS-11A conductivity meter. ^1H NMR spectra were measured on a Varian VR 300-MHz spectrometer, using TMS as a reference in $(CD_3)_2CO$ for (H_3L) and DMSO-d_6 for the La(III) complex. Mass spectra were performed on a VG ZAB-HS (FAB) instrument. The fluorescence spectra were recorded on a Hitachi RF-4500 spectrofluorophotometer.

5.3. Preparation of ligand (H_3L)

Naringenin (2.72 g, 10 mmol) and benzoyl hydrazine (1.37 g, 11 mmol) were dissolved in ethanol (40 mL). Acetic acid (1.0 mL) was added to this solution. The solution was refluxed on a water bath for one day with stirring. After that, the yellow solution was concentrated and cooled, a yellow solid separating out. The yellow precipitate was filtered, washed with water, and recrystallized from ethanol to give the ligand. Yield: 2.34 g (60%). Mp 231–232 °C. FAB-MS: $m/z = 391$ $[M+H]^+$. Anal. Calcd for $C_{22}H_{18}O_5N_2$: C, 67.69; H, 4.62; N, 7.18. Found: C, 67.29; H, 4.59; N, 7.20. IR $\nu_{max}(cm^{-1})$: $\nu_{C=O}$: 1640, $\nu_{C=N}$: 1600 cm^{-1}, ν_{NH}: 3205, δ_{NNH}: 1520.

5.4. Preparation of complex

The ligand (1.0 mmol, 0.390 g) was dissolved in ethanol (20 mL) and triethylamine (1.0 mmol, 0.102 g) was then added. After 5 min, $La(NO_3)_3{\cdot}6H_2O$ (0.5 mmol, 0.217 g) was added quickly and the solution was stirred for 10 h at room temperature. A yellow precipitate, the La(III) complex, was separated from the solution by suction filtration, purified by washing several times with ethanol, and dried for 24 h in vacuo. Anal. Calcd for $LaC_{44}H_{42}N_5O_{16}$: C, 51.01; H, 4.09; N, 6.76; La, 13.42. Found: C, 50.94; H, 3.99; N, 6.56; La, 13.22. IR $\nu_{max}(cm^{-1})$: $\nu_{C=O}$: 1609, $\nu_{C=N}$: 1570 cm^{-1}, ν_{NH}: 3228, δ_{NNH}: 1543, δ_{HOH}: 1594, ν_{NO3}: 1489, 1311, 1158, 893. Thermal analysis: $T = 58.4$ °C (H_2O loss: 5.45, calcd: 5.21).

5.5. Electronic spectra

Absorption titration experiments were performed with fixed concentrations of the drugs (10 μM) while gradually increasing the concentration of DNA. While measuring the absorption spectra, an equal amount of DNA

was added to both the compound solution and the reference solution to eliminate the absorbance of DNA itself.

5.6. Fluorescence spectra

To compare quantitatively the affinity of the compound bound to DNA, the intrinsic binding constants K_b of the two compounds to DNA were obtained by the luminescence titration method. Fixed amounts of compound were titrated with increasing amounts of DNA, over a range of DNA concentrations from 2.5 to 37.5 μM. An excitation wavelength of 352 nm was used, and total fluorescence emission intensity was monitored at 446 nm. The concentration of the bound compound was calculated using Eq. 1:[44]

$$C_b = C_t[(F - F^0)/(F^{max} - F^0)], \quad (1)$$

where C_t is the total compound concentration, F is the observed fluorescence emission intensity at given DNA concentration, F^0 is the intensity in the absence of DNA, and F^{max} is the fluorescence of the totally bound compound. Binding data were cast into the form of a Scatchard plot[53] of r/C_f versus r, where r is the binding ratio $C_b/[DNA]_t$ and C_f is the free ligand concentration. All experiments were conducted at 20 °C in a buffer containing 5 mM Tris–HCl (pH 7.1) and 50 mM NaCl concentrations.

Further support for the La(III) complex and ligand binding to DNA via intercalation is given through the emission quenching experiment. EB is a common fluorescent probe for DNA structure and has been employed in examinations of the mode and process of metal complex binding to DNA.[54] A 2-mL solution of 10 μM DNA and 0.33 μM EB (at saturating binding levels[38]) was titrated by 5–30 μM La(III) complex and ligand (λ_{ex} = 500 nm, λ_{em} = 520.0–650.0 nm). According to the classical Stern–Volmer equation:[55]

$$F_0/F = K_q[Q] + 1,$$

where F_0 is the emission intensity in the absence of quencher, F is the emission intensity in the presence of quencher, K_q is the quenching constant, and [Q] is the quencher concentration. The shape of Stern–Volmer plots can be used to characterize the quenching as being predominantly dynamic or static. Plots of F_0/F versus [Q] appear to be linear and K_q depends on temperature.

5.7. Viscosity measurements

Viscosity experiments were conducted on an Ubbdlodhe viscometer, immersed in a thermostatic water bath maintained to 25.0 °C. Titrations were performed for the La(III) complex and the ligand (0.5–3 μM), and each compound was introduced into a DNA solution (5 μM) present in the viscometer. Data were presented as $(\eta/\eta_0)^{1/3}$ versus the ratio of the concentration of the compound and DNA, where η is the viscosity of DNA in the presence of compound and η_0 is the viscosity of DNA alone. Viscosity values were calculated from the observed flow time of DNA containing solution corrected from the flow time of buffer alone (t_0), $\eta = t - t_0$.[48,56]

5.8. Cytotoxicity assay

Tumor cell lines used in this work were grown in RPMI-1640 medium supplemented with 10% (vol/vol) calf serum, 2 mmol^{-1} glutamine, 100 U mL^{-1} penicillin (U = 1 unit of activity), and 100 μg mL^{-1} streptomycin (GIBCO, Grand Island, NY) at 310 K under 5% CO_2. Cells in 100 μL culture medium were seeded into 96-well plates (Falcon, CA).

For human leukemia HL-60 cell, the microculture MTT [3-(4,5-dimethyl-2-thiazoyl)-2,5-diphenyl-2*H*-tetrazolium bromide] assay[57] was conducted as follows. The HL-60 cells were treated with compounds in a concentration gradient to give final concentrations at 1×10^{-5}, 1×10^{-6}, 1×10^{-7}, 1×10^{-8}, 1×10^{-9}, and 1×10^{-10} M, respectively. A 20 μL aliquot of MTT solution (5 mg/mL) was added directly to all the appropriate wells. The culture was then incubated for 4 h. A 50 μL of mixture solution composed of SDS [$CH_3(CH_{211}OSO_3Na$] 50(%), isobutyl acohol 5(%), and hydrochloride (0.01 mol mL^{-1}) was added to the system. After the plates were incubated overnight, the optical densities were read on a plate reader (model VERSA Max, Molecular Devices) at 570 nm.

For lung adenocarinoma A-549 cell, the growth inhibition was analyzed by the SRB (sulforhodamine B) assay.[58] Simply, following the treatment with the compound for 72 h, the cell cultures were fixed with 10% trichloroacetic acid and incubated for 60 min at 277 K. Then, the plates were washed and dried, SRB solution (0.4% wt/vol in 1% acetic acid) was added and the culture was incubated for an additional 15 min. After the plates were washed and dried, bound stain was solubilized with Tris buffer, and the optical densities were read on the same plate reader at 515 nm. The growth inhibitory rate of treated cells was calculated by $(OD_{control} - OD_{test})/OD_{control} \times 100\%$.

Acknowledgment

This work is supported by the National Natural Science Foundation of China 20475023) and Gansu NSF.

Supplementary data

Supplementary data associated with this article can be found in the online version at doi:10.1016/j.bmc.2005.10.031.

References and notes

1. Li, V. S.; Choi, D.; Wang, Z.; Jimenez, L. S.; Tang, M. S.; Kohn, H. *J. Am. Chem. Soc.* **1996**, *18*, 2326–2331.
2. Zuber, G.; Quada, J. C., Jr.; Hecht, S. M. *J. Am. Chem. Soc.* **1998**, *120*, 9368–9369.
3. Hecht, S. M. *J. Nat. Prod.* **2000**, *63*, 158–168.
4. Erkkila, K. E.; Odom, D. T.; Barton, J. K. *Chem. Rev.* **1999**, *99*, 2777–2796.

5. Metcalfe, C.; Thomas, J. A. *Chem. Soc. Rev.* **2003**, *32*, 215–224.
6. Haq, I.; Lincoln, P.; Suh, D.; Norden, B.; Choedhry, B. Z.; Chaires, J. B. *J. Am. Chem. Soc.* **1995**, *117*, 4788–4796.
7. Arturo, S.; Giampaolo, B.; Giuseppe, R.; Maria, L. G.; Salvatore, T. *J. Inorg. Biochem.* **2004**, *98*, 589–594.
8. Maribel, N.; Efrén José, C. F.; Anibal, S.; Mercedes, F. M.; Pedro, S.; Dwight, A.; Edgar, M. *J. Biol. Inorg. Chem.* **2003**, *8*, 401–408.
9. Catherine, H.; Marguerite, P.; Michael, R.; Heinz Stéphanie, G. S.; Bernard, M. *J. Biol. Inorg. Chem.* **2001**, *6*, 14.
10. Kumar, C. V.; Barton, J. K.; Turro, N. J. *J. Am. Chem. Soc.* **1985**, *107*, 5518–5523.
11. Xu, H.; Zheng, K. C.; Deng, H.; Lin, L. J.; Zhang, Q. L.; Ji, L. N. *Dalton. Trans.* **2003**, *3*, 2260–2268.
12. Mahadevan, S.; Palaniandavar, M. *Inorg. Chim. Acta* **1997**, *254*, 291–302.
13. Xu, H.; Zheng, K. C.; Deng, H.; Lin, L. J.; Zhang, Q. L.; Ji, L. N. *New J. Chem.* **2003**, *27*, 1255–1263.
14. Mozaar, A.; Elham, S.; Bijan, R.; Leila, H. *New J. Chem.* **2004**, *28*, 1227–1234.
15. Chaires, J. B. *Biopolymers* **1998**, *44*, 201–215.
16. Knekt, P.; Jarvinen, R.; Seppanen, R.; Heliovaara, M.; Pukkala, L. T.; Aromaa, A. *Am. J. Epidemiol.* **1997**, *146*, 223–230.
17. Sakaguchi, Y.; Maehara, Y.; Baba, H.; Kusumoto, T.; Sugimachi, K.; Newmanv, R. A. *Cancer Res.* **1992**, *52*, 3306–3309.
18. Habtemariam, S. *J. Nat. Prod.* **1997**, *60*, 775–778.
19. Aljancic, I.; Vajs, V.; Menkovic, N.; Karadzic, I.; Juranic, N.; Milosavljevic, S.; Macura, S. *J. Nat. Prod.* **1999**, *62*, 909–911.
20. Ko, F.; Chu, C.; Lin, C.; Chang, C.; Teng, C. *Biochim. Biophys. Acta* **1998**, *1389*, 81–90.
21. Nkengfack, A.; Vouffo, T.; Fomun, Z.; Meyer, M.; Bergendorff, S. O. *Phytochemistry* **1994**, *36*, 1047–1051.
22. Song, Y. M.; Kang, J. W.; Wang, Z. H.; Lu, X. O.; Gao, J. Z.; Wang, L. F. J. *Inorg. Biochem.* **2002**, *91*, 470–474.
23. Zhou, J.; Wang, L. F.; Tang, N. *J. Inorg. Biochem.* **2001**, *83*, 41–48.
24. Ramaswamy, A. S.; Jayaraman, S.; Sirsi, M.; Rao, K. H. *Indian J. Exp. Biol.* **1972**, 72–73.
25. Yu, S. Y.; Wang, S. X.; Luo, Q. H.; Wang, L. F.; Zhou, R. P.; Xing, G. *Polyhedron* **1993**, *12*, 1093–1096.
26. Padhy, S.; Kauffman, G. B. *Coord. Chem. Res.* **1985**, *63*, 127–160.
27. Wu, J. G.; Deng, R. W.; Chen, Z. N. *Trans. Met. Chem.* **1993**, *18*, 23–26.
28. Chandra, S.; Sharma, K. K. *Trans. Met. Chem.* **1984**, *9*, 1–3.
29. Yang, Z. Y.; Yang, R. D.; Li, Q.; Li, F. S. *Synth. React. Inorg. Met-Org. Chem.* **1999**, *29*, 205–214.
30. Yang, Z. Y. *Inorg. Met-Org. Chem.* **2000**, *30*, 1265–1272.
31. Geary, W. J. *Coord. Chem. Rev.* **1971**, *7*, 1–2.
32. Nagano, K.; Kinoshita, H.; Hirakawa, A. *Chem. Pharm. Bull.* **1964**, *12*, 1198–1206.
33. Narang, K. K.; Singh, V. P. *Transit. Met. Chem.* **1993**, *18*, 287–290.
34. Yang, Z. Y.; Yang, R. D.; Li, F. S.; Yu, K. B. *Polyhedron* **2000**, *19*, 2599–2604.
35. Nakamoto, K. *Infrared and Raman Spectra of Inorganic and Coordination Compounds*, 3rd ed.; Tohn Wiley: New York, 1978, p 227.
36. Zhen, Q. X.; Ye, B. H.; Zhang, Q. L.; Liu, J. G.; Ji, L. N.; Wang, L. *J. Inorg. Biochem.* **1999**, *76*, 47–53.
37. Yang, T.; Tu, C.; Zhang, J.; Lin, L.; Zhang, X.; Liu, Q.; Ding, J.; Xu, Q.; Guo, Z. *Dalton. Trans.* **2003**, *22*, 3419–3424.
38. Barton, J. K.; Danishefsky, A. T.; Golderg, J. M. *J. Am. Chem. Soc.* **1984**, *106*, 2172–2176.
39. Kelly, T. M.; Tossi, A. B.; McConnell, D. J.; Strekas, T. C. *Nucleic Acids Res.* **1985**, *13*, 6017–6034.
40. Tysoe, S. A.; Morgan, R. J.; Baker, A. D.; Strekas, T. C. *J. Phys. Chem.* **1993**, *97*, 1707–1711.
41. Pyle, A. M.; Rehmann, J. P.; Meshoyrer, R.; Kumar, N. J.; Turro, N. J.; Barton, J. K. *J. Am. Chem. Soc.* **1989**, *111*, 3053–3063.
42. Hiort, C.; Lincoln, P.; Nordén, B. *J. Am. Chem. Soc.* **1993**, *115*, 3448.
43. Wilson, W. D.; Ratmeyer, L.; Zhao, M.; Stekowski, L.; Boykin, D. *Biochemistry* **1993**, *32*, 4098–4104.
44. Satyanarayana, S.; Dabrowiak, J. C.; Chaires, J. B. *Biochemistry* **1992**, *31*, 9319–9324.
45. Boger, D. L.; Frink, B. E.; Brunette, S. R.; Tse, W. C.; Hedrick, M. P. *J. Am. Chem. Soc.* **2001**, *123*, 5878.
46. Zeng, Y. B.; Yang, N.; Liu, W. S.; Tang, N. *J. Inorg. Biochem.* **2003**, *97*, 258–264.
47. Kumar, C. V.; Barton, J. K.; Turro, N. J. *J. Am. Chem. Soc.* **1985**, *107*, 5518.
48. Michael, T. C.; Marisol, R.; Allen, J. B. *J. Am. Chem. Soc* **1989**, *111*, 8901–8911.
49. Xiong, Y.; He, X. F.; Zou, X. H.; Wu, J. Z.; Chen, X. M.; Ji, L. N.; Li, R. H.; Zhou, J. Y.; Yu, R. B. *J. Chem. Soc., Dalton Trans.* **1999**, *1*, 19–23.
50. Satyanarayana, S.; Dabrowiak, J. C.; Chaires, J. B. *Biochemistry* **1993**, *32*, 2573–2584.
51. Marmur, J. *J. Mol. Biol.* **1961**, *3*, 208.
52. Kumar, C. V.; Asuncion, E. H. *J. Am. Chem. Soc.* **1993**, *115*, 8547–8553.
53. Howe, G. M.; Wu, K. C.; Bauer, W. R. *Biochemistry* **1976**, *19*, 339–347.
54. Kumar, C. V.; Barton, J. K.; Turro, M. J. *J. Am. Chem. Soc.* **1985**, *107*, 5518–5523.
55. Efink, M. R.; Ghiron, C. A. *Anal. Biochem.* **1981**, *114*, 199–206.
56. Eriksson, M.; Leijon, M.; Hiort, C.; Norden, B.; Gradsland, A. *Bioccemistry* **1994**, *33*, 5031–5040; Xiong, Y.; He, X. F.; Zou, X. H.; Wu, J. Z.; Chen, X. M.; Ji, L. N.; Li, R. H.; Zhou, J. Y.; Yu, R. B. *J. Chem. Soc. Dalton Trans.* **1999**, *1*, 19–23.
57. Alley, M. C.; Scudiero, D. A.; Monks, A.; Hursay, M. L.; Czerwinski, M. J.; Fine, D.; Abbott, B. J.; Mayo, J. G.; Shoemaker, R. H.; Boyd, M. R. *Cancer Res.* **1988**, *48*, 589–601.
58. Skehan, P.; Storeng, R.; Scudiero, D.; Monks, A.; McMahon, J.; Vistica, D.; Warren, J. T.; Bokesch, H.; Kenney, S.; Boyd, M. R. *J. Natl. Cancer Inst.* **1990**, *82*, 1107–1112.